Identification of Potent and Selective RNA Antagonists of the IFN-γ-Inducible CXCL10 Chemokine†

Martin L. Marro,‡,§ Dion A. Daniels,*,‡ Anne McNamee,|| David P. Andrew,|| Trevor D. Chapman,⊥ Ming S. Jiang,▽ Zining Wu,▽ Janet L. Smith,§ Kalpana K. Patel,○ and Katy L. Gearing‡

Gene Expression and Protein Biochemistry, Computational, Analytical & Structural Sciences, Immunopharmacology, and Screening Sciences, GlaxoSmithKline Medicines Research Centre, Gunnels Wood Road, Stevenage, Herts SG1 2NY, United Kingdom, and Department of Assay Development and Compound Profiling, GlaxoSmithKline, 709 Swedeland Road, King of Prussia, Pennsylvania 19406

Received August 27, 2004; Revised Manuscript Received March 30, 2005

ABSTRACT: CXCL10 (also known as IP-10 in humans and CRG-2 in mice) is a nonglycosylated chemokine and a member of the non-ELR CXC chemokine subfamily implicated in a variety of inflammatory conditions. The role of CXCL10 in different disease states still requires clarification, and new approaches are necessary to better understand its biological function. We report here the isolation of a series of nuclease-resistant RNA aptamers that act to antagonize human CXCL10 function in a number of in vitro and cell-based assays. The two most potent aptamers identified were highly selective for human CXCL10. A further aptamer was identified that antagonized both the human and the mouse CXCL10. A combination of a molecular-biology-based truncation and solid-phase synthesis enabled the truncation of one of the aptamers from 71 to 34 nucleotides. This was followed by PEGylation, 3′ capping, and further stabilization of the RNA aptamer, while its high potency was maintained. These aptamers could be utilized as powerful target validation tools and may also have therapeutic potential. To our knowledge, the CXCL10 aptamers generated are the most potent antagonists of CXCL10/CXCR3 signaling reported to date.

CXCL10 is a 77 amino acid secreted nonglycosylated chemokine (*1*). The mature protein contains four cysteines, the first two of which are separated by one amino acid. It lacks the ELR sequence preceding the first cysteine, typical of CXCL8 and other CXC chemokines active on neutrophils, and hence, it is a member of the non-ELR CXC chemokine subfamily.

CXCL10 is involved in the activation and recruitment of leukocytes, as well as nonhematopoietic cells (*2*). It is expressed constitutively at low levels in thymic, splenic, and lymph node stroma (*3*). However, its expression can be induced by interferon γ (*4*) in a variety of cell types, including endothelial cells, keratinocytes, fibroblasts, mesangial cells, astrocytes, monocytes, and neutrophils (*5*). High expression has been noted in many Th1-type inflammatory conditions, including skin diseases (*6*−*8*), atherosclerosis (*9*), multiple sclerosis (*10*, *11*), and allograft rejection (*10*, *12*, *13*). hCXCL10[1] has been shown to have angiostatic (*14*−*17*) and antitumor activity (*18*, *19*). This chemokine might also have an important regulatory role in inflammatory bowel disease (*20*) and allergic response (*21*), and it has been recently demonstrated to stimulate HIV replication (*22*).

Chemokines activate leukocytes by binding to G-protein-coupled receptors. CXCL10 binds to the CXC chemokine receptor 3 (CXCR3), which can be activated by two further ligands, interferon-inducible T cell-α chemoattractant (CXCL11) and monokine induced by γ-interferon (CXCL9) (*23*). The CXCR3 binding chemokines are unique in their ability to bind receptors from both the CC and CXC classes of chemokine receptors (*24*).

A review of the approaches taken for target validation of chemokines and their receptors has been reported recently (*25*), and the role of CXCL10 in different disease states still requires clarification. Although some CXCL10 knockout models (*26*) and neutralization antibody studies have been reported (*20*, *21*, *27*−*29*), new chemical, biochemical, and biological approaches are still required to further validate this target. The goal of these studies was to generate novel antagonists that could be used to better understand the biological function of CXCL10.

In view of the advances in SELEX methodology (*30*, *31*) and reports demonstrating the successful generation of

† M.L.M. was a recipient of a postdoctoral Marie Curie Industry Host Fellowship (EU).

* To whom correspondence should be addressed. Phone: +44-1438-764086. Fax: +44-1438-764865. E-mail: dion.a.daniels@gsk.com.

‡ Gene Expression and Protein Biochemistry, GlaxoSmithKline Medicines Research Centre.

§ Current address: Wolfson Institute for Biomedical Research, University College London, Cruciform Building, Gower St., London WC1E 6AE, U.K.

|| Immunopharmacology, GlaxoSmithKline Medicines Research Centre.

⊥ Computational, Analytical & Structural Sciences, GlaxoSmithKline Medicines Research Centre.

▽ Department of Assay Development and Compound Profiling, GlaxoSmithKline.

○ Screening Sciences, GlaxoSmithKline Medicines Research Centre.

[1] Abbreviations: hCXCL10, human CXCL10 (IP-10); mCXCL10, mouse CXCL10 (CRG-2); PEG, polyethylene glycol; N6, $NH_2(CH_2)_6$, a 5′ linker; idT, inverted deoxythymidine, a 3′ CAP; SELEX, systematic evolution of ligands by exponential enrichment; IL, interleukin; IFN, interferon; RBL, rat basophilic leukemia; CHO, Chinese hamster ovary; FCS, fetal calf serum; FLIPR, fluorometric imaging plate reader; GAGs, glycosaminoglycans.

10.1021/bi048145w CCC: $30.25
Published on Web 05/21/2005

Table 1: Protein/RNA Amounts Used during Each Round of the SELEX Experiment

round of SELEX	amt of hCXCL10 or mCXCL10 added (μL)	amt of RNA added (pmol)	binding time (min)	no. of postbinding washes
1	50	1100	30	5
2	25	100	30	6
3	10	100	30	8
4	5	100	30	10
5	2.5	100	15	12[a]
6	2.5	100	15	12

[a] 5 min per wash.

aptamers against proteins, this procedure was used to generate nuclease-resistant RNA antagonists to CXCL10. The methodology is an in vitro protocol in which single-stranded oligonucleotides are selected from DNA or RNA combinatorial libraries of $\sim 10^{15}$ different sequences, on the basis of binding affinity at a target protein or other molecule (*30*, *32*). Several cycles of exposure to the target, selection, and amplification are performed until the target-specific sequences dominate the population. Since their discovery in 1990 (*30*, *33*), aptamers have been generated against a wide variety of targets (*34*, *35*). The selected aptamers have demonstrated very good affinity and specificity for their targets, and a number of them have been shown to be biologically active both in vitro (*36*, *37*) and in vivo (*38*). We report here the isolation of a series of RNA aptamers with high binding affinity for human and/or mouse CXCL10 that act to antagonize its function in a number of in vitro and cell-based assays. These aptamers could be utilized as powerful target validation tools and may also have therapeutic potential. To our knowledge, the CXCL10 aptamers generated are the most potent antagonists of CXCL10/CXCR3 signaling reported to date.

EXPERIMENTAL PROCEDURES

Materials. Human and mouse CXCL10, human CCL1, CCL22, IL-2, IL-4, IL-7, and IL-12, and the anti-CCL1 antibody were purchased from R&D Systems, Europe Ltd. (Abingdon, Oxon, U.K.). Human and mouse CXCL11 and CXCL9 were purchased from Peprotech (London, U.K.). The anti-IL-12, anti-IL-4, anti-IFN-γ, anti-CD3, anti-CD28, and anti-CD95L antibodies were purchased from Pharmingen, BD Biosciences (Oxford, U.K.). Forskolin was purchased from Sigma-Aldrich (Poole, Dorset, U.K.).

SELEX. Iterative rounds of selection and amplification were performed as described (*37*) with minor modifications. Human and mouse CXCL10 (3 μg/μL) were diluted to the required concentration in SCHMK buffer (110 mM NaCl, 1 mM $MgCl_2$, 20 mM HEPES, pH 7.0, 1 mM $CaCl_2$, 5 mM KCl) and incubated with 100 μL of Dynal beads overnight at 4 °C to allow hydrophobic bead binding, and SELEX stringency was applied as described (*39*). For each SELEX round, RNA, diluted in 50 μL of wash buffer, was added to the beads in individual Eppendorf tubes at the amounts shown in Table 1. The tubes were incubated at 37 °C for 30 min, after which individual samples were washed to remove unbound RNA. To elute specifically bound RNA, 20 μL of 3 N7 primer (5 pmol/μL) was added to individual tubes and the mixture heated at 95 °C for 3 min and then left at room temperature (rt) for 5 min. Reverse transcription of the eluted RNA was then carried out in the presence of the beads, and the supernatant was transferred to a fresh tube. PCR and in vitro transcription were then performed to generate RNA for the next round of SELEX as described previously (*31*). 2′-Fluoropyrimidines were used in the selection because they are known to impart a greater level of RNA stability, making the transcribed material stable enough to be used in cell culture assays.

Aptamer−Chemokine Binding Assays. Binding assays were carried out by nitrocellulose filter partitioning as described (*31*).

Cloning and Sequencing. Aptamer DNA was cloned into the plasmid pCR2.1 using the TA cloning kit (Invitrogen) according to the manufacturer's instructions. Plasmid clones were purified and sequenced, and the sequences derived from both SELEX experiments (hCXCL10 and mCXCL10) were aligned using the Clustal software package of the GCG suite of molecular biology programs.

Oligonucleotide Synthesis. Synthesis of full-length RNAs was performed by in vitro transcription of synthetic DNA templates and purification by denaturing gel electrophoresis, as described (*31*). 2′-Fluoropyrimidines (aimed to increase endonuclease resistance; Trilink BioTechnologies Inc., San Diego, CA) and 2′-hydroxypurines (Roche Molecular Biochemicals, Mannheim, Germany) were used in each case.

Truncated RNAs were synthesized either biologically using in vitro transcription and purified by denaturing gel electrophoresis (aptamer C44-47) or chemically (aptamers C44-34 and C44-38), gel-purified, and deprotected (Dharmacon Research, Lafayette, CO). 2′-Fluoropyrimidines and 2′-hydroxypurines were also used in each case. Serial 5′ and 3′ truncations in five nucleotide steps were carried out by PCR, amplification, and in vitro transcription (Figure 5). Since 5′ PCR primers for aptamer generation usually contain the T7 RNA polymerase promoter, a strategy was designed to ensure that each of the 5′ nested primers would allow initiation of the in vitro transcription reaction. To achieve this, a region containing +1−6 nucleotides of the T7 RNA polymerase transcription start site (GGAGA) was added to the 5′ end of each 5′ primer as shown in Figure 5. This approach generated a total of 49 possible truncations. A rational approach using secondary structure predictions (see below) for each possible truncate simplified the screening procedure to only 15 different truncated C44 forms (data not shown) which were synthesized by PCR followed by in vitro transcription and purification.

Cell Lines. The stable RBL cell line expressing human CXCR3 was generated and maintained in DMEM/F-12 medium supplemented with 10% FCS, 2 mM L-glutamine, and 0.8 mg/mL G418 (Life Technologies).

A CHO-K1 cell line coexpressing the human CCR8 (Euroscreen) and Gq proteins was generated and maintained in DMEM/F-12 medium supplemented with 10% FCS, 1 mg/mL G418, and 0.4 mg/mL hygromycin B.

A CHO cell line coexpressing human CXCR3 and Gα16 (Euroscreen) was generated and maintained in DMEM/F-12 high-glucose medium supplemented with 10% FCS, 15 mM HEPES, and 2 mM L-glutamine (Life Technologies).

cAMP Assay. A HitHunter cAMP assay kit (EFC Chemiluminescent Detection) for suspension cells was used to detect cAMP levels (DiscoveRx, Fremont, CA). Prior to the aptamer experiment, dose-dependent induction of cAMP by

forskolin was measured. The activity of hCXCL10 required to inhibit forskolin-induced cAMP production was then measured by incubating cells with hCXCL10 for 30 min prior to the addition of forskolin. The EC_{50} and EC_{70} values of hCXCL10 were determined for each experiment. Cells were washed and resuspended in culture medium without FCS at a density of 6×10^6 cells/mL. After 30 min of incubation of aptamer/CXCL10 mixtures at 37 °C, a 5 μL sample of the cells was added to each well, and the resulting mixtures were incubated at 37 °C for 60 min. A 5 μL sample of forskolin (a final concentration of 10 μM at around EC_{50}) was then added, and the resulting mixtures were incubated at 37 °C for another 30 min. HitHunter cAMP assay reagents were then added according to the manufacturer's instructions. The luminescent signal was read in a Viewlux imager (Perkin-Elmer). The data were normalized to the percentage of maximum hCXCL10 activity in the absence of aptamers.

Secondary Structure Prediction of RNA Aptamers. Secondary structures of individual aptamers were predicted using the MFOLD program (*40*).

Assay for hCXCL10 or mCXCL10 Binding to Heparin, Measured by Surface Plasmon Resonance. Surface plasmon resonance measurements were conducted using a BIAcore 2000 instrument as described (*37*). The inhibitory effects of preincubating aptamers with the chemokine (200 nM) for 30 min at rt prior to injection were observed, and the reduction in maximum binding response was calculated as a percentage of that of random control aptamer responses.

FLIPR Assays. A microtiter plate based calcium mobilization FLIPR assay (*41*) was conducted as described (*37*) with the following modifications. Cells were plated at a density of 3×10^5 cells/mL into black 96-well viewplates (Packard Biosciences) 24 h prior to the assay. The cell medium was removed, and the cells were loaded with 100 μL of 1 μM Fluo 4AM (Molecular Probes) in FLIPR buffer (10 mM HEPES, 10 mM glucose, 3 mM probenecid, 145 mM NaCl, 5 mM KCl, 2 mM $CaCl_2$, 1 mM $MgCl_2$). Following 1 h of incubation, the cells were washed with 100 μL of the same buffer without dye and probenecid, and 100 μL of buffer was then added to each well. A 50 μL sample of chemokine (at EC_{50-70} final concentration) $\pm$ aptamer was added. The plates were read every 1 s for 1 min on an FLIPR (Molecular Devices, Sunnyvale, CA), with the agonist added at 5 s. Concentration−response curves or single agonist responses were generated by calculating peak fluorescence counts above background and normalized according to basal values. For agonist responses to chemokine in the presence/absence of aptamer, agonist was incubated with aptamer/buffer for 30 min at rt prior to addition to the cells. The EC_{50} and EC_{70} values were determined prior to each aptamer experiment. Each point represents the mean and standard error of three replicate wells.

Preparation of Chronically Activated Human Th1 and Th2 Lymphocytes. The preparation of activated Th1 and Th2 cells was carried out as described (*42*) with several modifications. Umbilical cord CD4 lymphocytes (Poietic Systems, Germantown, MD) were cultured in complete RPMI medium with 10% FCS and 10 ng/mL IL-2 overnight. A total of 1×10^6 cells/mL were plated out into plates coated with anti-CD3 and anti-CD28 antibodies at 5 μg/mL, in either Th1 medium [complete RPMI medium with IL-2 plus 10 ng/mL IL-12 and 1 μg/mL anti-IL-4 antibody (Pharmingen)] or Th2 medium [complete RPMI medium with IL-2, plus 10 ng/mL IL-4 and 1 μg/mL anti-IFN-γ antibody (Pharmingen)]. The Th1 and Th2 directed cord blood cells were stimulated for 4−6 days at 37 °C in a CO_2 incubator until the cells were confluent. The cells were washed twice and transferred to a flask at 0.5×10^6 cells/mL in complete RPMI plus IL-2 (10 ng/mL) and IL-7 (5 ng/mL). After a rest period of 4−7 days these once-stimulated cells were frozen down as primary activated stocks or restimulated as secondary activated cells, rested for 5−6 days, and used in the chemotaxis assays. For the second activation phase, anti-CD95L (2 μg/mL) was added to Th1 and Th2 media, to prevent apoptosis.

Chemotaxis Assay. This assay was performed as described (*37*) with the following modifications. Th cells were washed once in PBS and resuspended in chemotaxis buffer (RPMI, 2% FCS, 10 mM Hepes) at 5×10^6 cells/mL. Chemotaxis chambers (96-well) fitted with a 3 μm pore polycarbonate filter (Receptor Technologies Ltd., Adderbury, Oxon, U.K.) were used. Aptamer and chemoattractant were preincubated for 30 min at rt in chemotaxis buffer, and then 30 μL was transferred to the bottom well of the chemotaxis plate. A 50 μL sample of Th cells, washed once in PBS and resuspended in chemotaxis buffer at 5×10^6 cells/mL, was placed on top of the filter above each well. After 1−2 h of incubation, the cells of the bottom well were transferred to a 96-well flat-bottom plate. The wells were washed once with 60 μL of chemotaxis buffer, and this was also transferred to the 96-well flat-bottom plate. A 10 μL sample of Alamar Blue (Serotec Ltd., Kidlington, Oxford, U.K.) in PBS was finally added to each well of the flat-bottom plate. After 17−18 h, the plate was read on a Cytofluor II fluorescent plate reader (Applied Biosystems, Warrington, Cheshire, U.K.) at 530 nM (excitation) and 590 nM (emission). The same assay was carried out for both Th1 and Th2 cells. Each point represents the mean and standard error of three replicate wells.

Data Analysis. Dissociation constants (K_d) and EC_{50} and IC_{50} values were determined by fitting the data using Prism 3.0 or Robosage Microsoft Excel add-in software.

RESULTS

SELEX. Nuclease-resistant and high-affinity RNA ligands to human and mouse CXCL10 were generated independently by six iterative rounds of SELEX, using the conditions described in Table 1. To ensure the isolation of high-affinity aptamers, the stringency of the SELEX procedure was increased in later rounds by reducing the amount of protein and RNA, reducing the binding time, and increasing the stringency of postbinding washes in the experiment (*39*). As there was no significant change in the apparent affinity of the last RNA pools, the SELEX was assumed to have reached completion. The round 6 pool was cloned, and 50 individual aptamer clones derived from both hCXCL10 and mCXCL10 SELEX experiments were sequenced. Aptamers in this study have a core variable region (40 bases) and 5′- and 3′-terminal regions of 15 and 16 bases, respectively. An alignment of the aptamer variable regions led to the identification of six sequence families along with a number of "orphan" sequences that were only represented once in the final pools (Figure 1).

Aptamer	Sequence	Family	Assayed (binding)
P7	.TCCCAACAT ACTGAACGAT GCCACAACCC ...TCACTCC CCCT.....	Orphan	*
P17	CCACCAACAC ACTGCATAA. .ACAGAACC. ...TCATCCC CCTGCC....	Orphan	*
P32	.CTCAAGCAT TTC......A TTCCCCATCA GTCCCACGCA GCCCT.....	Orphan	*
P25	...GAAACCT TTTGAGAAAA GCCCCCACCA .TCCCAT.CA CCCCT.....	Orphan	*
C2	..TCTAGTCG ATAATTCTGC CCAAGACATC CTTCCTCTTG CC.....	I	
C17	..TCTAGTCG ATAATTCTGC CCAAGACATC CTTCCTCTTG CC.....	I	
P27	..TCTAGTCG ATAATTCTGC CCAAGACATC CTTCCTCTTG CC.....	I	
C24	..TCTAGTCG ATAATTCTGC CCAAGACATC CTTCCTCTTG CC.....	I	*
C27	..TCTAGTCG ATAATTCTGC CCAAGACATC CTTCCTCTTG CC.....	I	
C13	..TCTAGTCG ATAATTCTGC CCAAGACATC CTTCCTCTTG CC.....	I	
P38	..TCTAGTCG ATAATTCTGC CCAAGACATC CTTTCTCTTG CC.....	I	*
C30	..TCTAGTCG ATAATTCTGC CCAAGACATC CTTCCTCTTG CT.....	I	*
C23	.... .CAACTCTCC CCTACCTCCC CTTCTTCTTC CTCCCTCGCTG	Orphan	*
C11	....GACCCGAC ACATCCAGTA CTTCCTCTCC TTCACTGCCC	Orphan	*
C44	**....CATGCG TCTGACCTAC GTGCCAAGCA TTTGTGTAAC CCGT.....**	**Orphan**	*
P1	......ACTG AACGATATCC TTGGCGCGCA TC.GCGTATC CCCTGCT...	Orphan	*
P18	AAACGAGCCA AAAGTGGAAG CCTCA..CTG CAAACCTCGT CCC.....	II	*
P34	AAACGAGCCA AAAGTGGAAG CCTCA..C.G CAAACCTCGT CCC.....	II	*
P6	AAACGAGCCA AATGTGGAAG CCTCA..C.G CAAACCTCGT CCC.....	II	*
P2	.... TCCGTAGAAT CCTTAACCTG CAAACATGAC TCCCCTGGT.	Orphan	*
P15	....AAGACT CACATAAAAA CCCGGAAACG AGCCTACTCT CCCCCC.	Orphan	*
P16	........TC CAGGAAAGCA CCCCAGTGTC ACTCCATCAT AGGCGCCT..	Orphan	*
C42	.....TGACT CCTCTGA.CA GCCTAATTTT CCCCGATTAC CCTG.....	III	
C18	.....TGACT CCTCTGA.CA GCCTAATTTT CCCCGATTAC CCTG.....	III	*
C22	.....TGACT CCTCTGA.CA GCCTAATTTC TCCCGATTAC CCTG.....	III	*
P26	...GAGGTCT CACGCTT.GT AACGAGCCTG TCTTCATCCT CCCT.....	Orphan	*
P48	....AAGACT CACAGT..GA AACGAGCCGC TCATCTTCTG CCGGCC....	Orphan	*
P19	...TGACT.T CGTTCTGGCC .CTCTGTATT TT.CCATACA CTGCCC....	IV	
C38	...TGACT.T CGTTCTGGCC .CTCTGTATT TT.CCATACA CTGCCC....	IV	*
C15	...TGACT.T CGTTCTGGCC .CTCTGTATT TT.CCATACA CTGCCC....	IV	
C40	....GCCTCT CGATCTGCCC .ATTCGTATC GTATTACGCA CTGCC.....	Orphan	*
P47	....AGTTCT CAGGCTGAGC .CCATACGAC CTTCCCTCTG GCCCCT....	Orphan	*
P30	.....TTTCA CAGGCTGGAC ATCGCATGTA CGTCCTTGCA TGCCT.....	Orphan	*
C32	....TCGACT CGTATTGCCC ATAGTCATTC CTTTCCCCTA TGCC.....	V	
C16	....TCGACT CGTATTGCCC ATAGTCATTC CTCTCCCCTA TGCC.....	V	*
C21	....TCGACT CGTATTGCCC ATAGTCATTC CTTTCCCCTA TGCC.....	V	
C31	....TCGACT CGTATTGCCC ATAGTCATTC CTTTCCCCTA TGCC.....	V	*
C6	....TCGACT CGTATTGCCC ATAGNCATTC CTTTCCCCTA TGCC.....	V	
C7	.....TGACT TGTCTGGCTC CTTTTGTACC CTTCCCCAAT TGCCC.....	Orphan	*
P28	......AGTT TCTTCTGAGG TCTGAACCTT TCCGAAAGCT GGCGCT....	VI	
P24	......AGTT TCTTCTGAGG TCTGAACCTT TCCGAAAGCT GGCGCT....	VI	*
P22	......AGTT TCTTCTGAGG TCTGAACCTT TCCGAAAGCT GGCGCT....	VI	
P31	**......AGTT TCTTCTGAGG TCTGAACCTT TC.GAAAGCT GGCGCT...**	**VI**	*
P12	**..ACTGAACC TAATTTGAAA T.TGGCTGGC GCGCATATTC CGT.....**	**Orphan**	*
P13	........CT AAACTTGTAA TTTGCCGATG AAACCTAGAC TCCCCGGT..	Orphan	*
P10	...AAATTCC CTAACCATAG TTAGGCCACA GAACTCCGCG CCT.....	Orphan	*
C20	.......GTC CCTTCCAAAT ATCACTCTCA CATCGAGTAC CCGCCCT...	Orphan	*
P37	...TGACTCC TCCCCAACTC ATTGCAGCTA GCTCCATTGC CCC.....	Orphan	*
P29	.......GCT TTTCCTGACT AAGTGGGCTC ATCCTAACCC CACCCT....	Orphan	*

FIGURE 1: Sequence of aptamer clones. The 40N variable region of each DNA clone is illustrated. Sequences were aligned and grouped into sequence families and orphans. An asterisk indicates one representative of each sequence group characterized in a nitrocellulose binding assay. "P" aptamers were generated by the hCXCL10 SELEX, whereas "C" aptamers were generated by the mCXCL10 SELEX. The highest affinity aptamers for hCXCL10 or mCXCL10 are in boldface type.

Binding of the Anti-hCXCL10 and Anti-mCXCL10 Aptamers to Their Chemokine Targets. To characterize individual aptamers, RNA was made from 36 representative clones (indicated in Figure 1) and the relative binding of each of

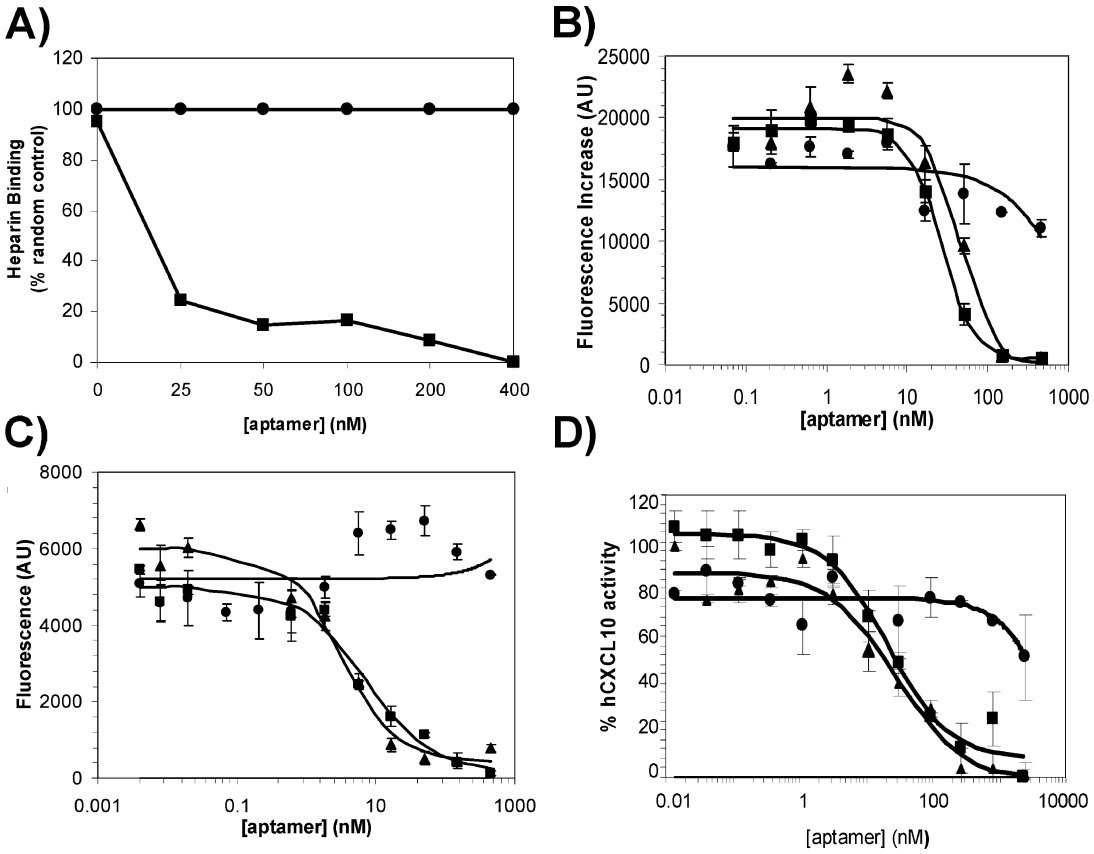

FIGURE 2: Functional characterization of anti-hCXCL10 aptamers. P12 (▲), P31 (■), and a random aptamer control (●) are shown. (A) Aptamer blockade of heparin binding to hCXCL10 in vitro by using surface plasmon resonance. P31 showed a dose-dependent heparin binding inhibition. Each point represents the sensorgram peak as a percentage of the random control value. (B) Aptamer inhibition of calcium mobilization in RBL cells expressing human CXCR3. (C) Aptamer antagonism of hCXCL10-induced chemotaxis in human Th1 cells. (D) Inhibition of hCXCL10 activity by aptamers in a cAMP assay. In all these assays, a dose-dependent inhibition is shown with P12 and P31 aptamers but not with the random aptamer. (B−D) experiments were carried out in triplicate. Error bars represent SE.

the family-derived or orphan-derived RNAs to the corresponding chemokine target (25 nM) was determined in an RNA binding assay by using nitrocellulose filter partitioning. The affinities of 12 anti-hCXCL10 and 11 anti-mCXCL10 aptamers were then determined in nitrocellulose binding assays. P12 and P31 (Figure 1, boldface) were found to be the highest affinity anti-hCXCL10 aptamers (1.76 and 1.53 nM, respectively) (Supporting Information, Figure 7). C44 (Figure 1, boldface) was found to be the highest affinity anti-mCXCL10 aptamer (3.5 nM) (data not shown). Further characterization focused on the functional behavior of the anti-hCXCL10 aptamers (P12/P31) and the anti-mCXCL10 aptamer (C44).

In Vitro Functional Characterization of Anti-hCXCL10 Aptamers. It has been postulated that GAGs on the cell bearing the seven transmembrane chemokine receptor facilitate ligand binding to its high-affinity receptor (*43*), while GAGs on endothelial cells and in the extracellular matrix might be important for retaining chemokines close to their site of secretion (*44*). GAGs might also be involved in the signaling of chemokines (*45*, *46*). CXCL10, like many chemokines, binds to cell surface GAGs (*15*, *47*, *48*). To determine if the high-affinity aptamers generated in this study were capable of functionally antagonizing hCXCL10, the ability of the aptamers to block the binding of hCXCL10 to heparin was measured using surface plasmon resonance (BIAcore). Both P12 (not shown) and P31 (Figure 2A) were able to functionally antagonize the binding of hCXCL10 to heparin in a dose-dependent fashion. The random control aptamer showed no activity (Figure 2A).

Cell-Based Functional Characterization of Anti-hCXCL10 Aptamers. The ability of P12 and P31 aptamers to antagonize hCXCL10-induced intracellular calcium mobilization was tested in an RBL cell line stably expressing the human CXCR3 receptor (Figure 2B). P12 and P31 aptamers but not a random control aptamer blocked this mobilization in a dose-dependent fashion. Additionally, P12 and P31 (but not the random control aptamer) also blocked hCXCL10-induced chemotaxis of human Th1 cells (Figure 2C). None of the aptamers had any effect on the fluorescent readout in either calcium mobilization or chemotaxis assays in the absence of hCXCL10 (data not shown).

A cAMP assay was used to further investigate the functional activity of these aptamers. The CXCR3 receptor is known to couple to Gi-type G-proteins. Activation of CXCR3 would lead to receptor-mediated inhibition of adenylyl cyclases. hCXCL10 activity was thus measured by its ability to inhibit forskolin-induced cAMP production. Figure 2D shows a dose-dependent inhibition of the hCXCL10 activity by the P31 and P12 aptamers. Further analyses revealed that the hCXCL10 agonist dose−response curve could be rightward shifted by the presence of increasing concentrations of P12 and P31 (Supporting Information, Figure 8).

Table 2 summarizes the affinities and potencies of the best anti-hCXCL10 aptamers in the binding assay and in different

Table 2: Affinities and Potencies of the Best Anti-hCXCL10 Aptamers in Different Binding and Functional Assays According to Figure 2 and the Supporting Information

	K_d (nM)	IC_{50} (nM)			
aptamer	nitrocellulose binding	heparin binding	calcium mobilization	chemotaxis	cAMP
(▲) P12	1.8	ND[a]	27.6	1.3	28.0
(■) P31	1.6	15	20.3	19.7	2.0
(●) random	–	–	–	–	–

[a] ND stands for not determined.

functional assays. A very good correlation of aptamer potencies between these assays was found.

Specificity of Anti-hCXCL10 Aptamers. hCXCL10 shares ~37% identity with hCXCL9 and hCXCL11, the other two IFN-γ-inducible non-ELR CXC ligands of the CXCR3 receptor. As can be seen in Figure 3A−C, P12, P31, and the random control aptamer did not specifically antagonize hCXCL9 or hCXCL11 function in a chemotaxis assay. The same result was observed in a calcium mobilization assay (data not shown). The observed high potency and specificity are in agreement with the expected properties of RNA aptamers.

It is known that hCXCL10 and mCXCL10 are functional across species, and this is in agreement with the high homology between amino acid sequences (70% identity). However, when P12 and P31 were tested against mCXCL10, they did not antagonize its function either in the calcium mobilization assay (Figure 3D) or in the heparin binding assay (data not shown), demonstrating the high level of selectivity for hCXCL10. The activity of P12 and P31 activity at nonrelated chemokines was also tested. P12 and P31 aptamers did not have any effect on hCCL1/CCR8-induced signaling in a calcium mobilization assay using CHO cells expressing the recombinant human CCR8 receptor (Supporting Information, Figure 9A). Additionally, the aptamers did not have any effect on hCCL22 chemokine in a chemotaxis assay using human Th2 cells (Supporting Information, Figure 9B). In summary, the anti-hCXCL10 aptamers demonstrated high specificity and selectivity by functionally antagonizing hCXCL10 but not mCXCL10, hCXCL9, hCXCL11, hCCL1, or hCCL22 chemokines.

C44 Aptamer: A Potent Antagonist against Both mCXCL10 and hCXCL10 Orthologues. The aptamers described above have been shown to be specific antagonists of hCXCL10. To better understand the biological function of CXCL10, aptamers to the murine orthologue have also been generated. C44, the highest affinity anti-mCXCL10 aptamer derived from the mCXCL10 SELEX, was found to block both mCXCL10 and hCXCL10 functional activities. As shown in Figure 4A, C44 blocked heparin binding both to mCXCL10 (left panel, $IC_{50} = 30-40$ nM) and to hCXCL10 (right panel, $IC_{50} = 34-40$ nM). When C44 aptamer was tested in a calcium mobilization assay using an RBL cell line expressing the human CXCR3 receptor, it was able to strongly antagonize mCXCL10 function ($IC_{50} = 37.0$ nM, Figure 4B, left panel) as well as hCXCL10 function (Figure 4B, right panel, $IC_{50} = 45.9$ nM). C44 was also tested in an hCXCL10-induced chemotaxis assay using human Th1 cells and displayed potency similar to those of the other two functional assays (Figure 4C, $IC_{50} = 20.2$ nM). In summary, the anti-

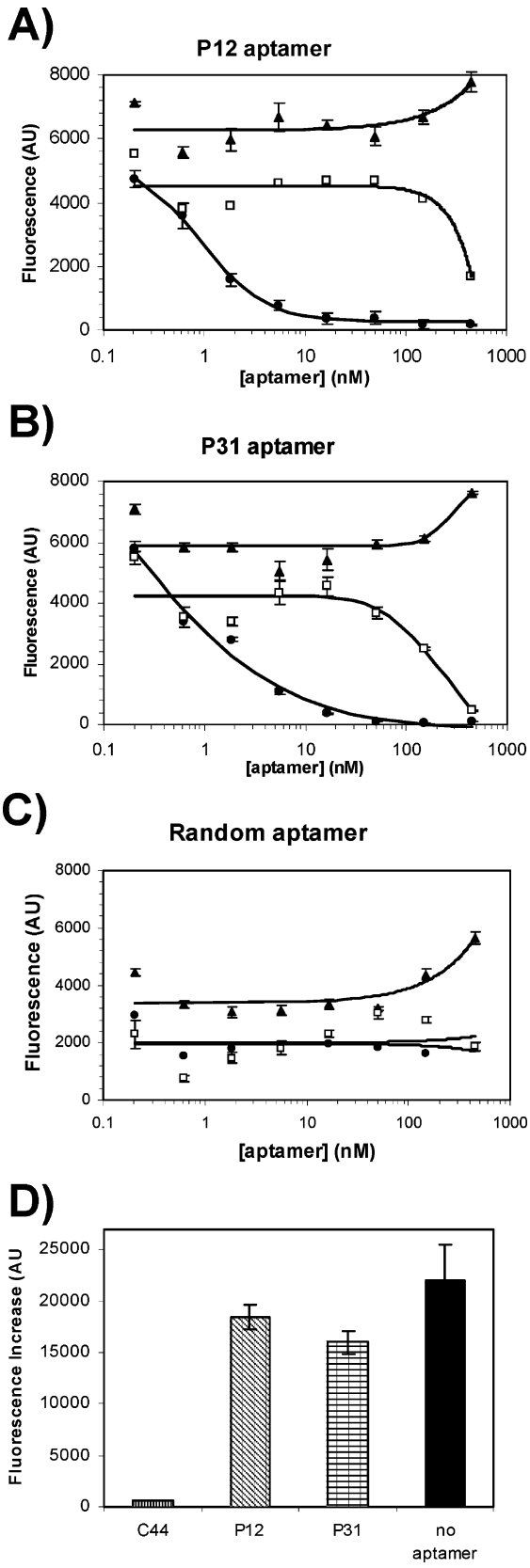

FIGURE 3: Specificity of anti-hCXCL10 aptamers. (A) P12 and P31 aptamers did not have any specific antagonistic effect on other hCXCR3 ligands (hCXCL9 and hCXCL11) in a human Th1 chemotaxis assay. hCXCL10 (●), hCXCL11 (▲), and hCXCL9 (□) curves are shown. (B) Anti-hCXCL10 aptamers did not show any effect on mCXCL10 in the calcium mobilization assay (150 nM aptamer). C44 depicts the anti-mCXCL10 aptamer used as a positive control described in Figure 4. All these experiments were carried out in triplicate. Error bars represent SE.

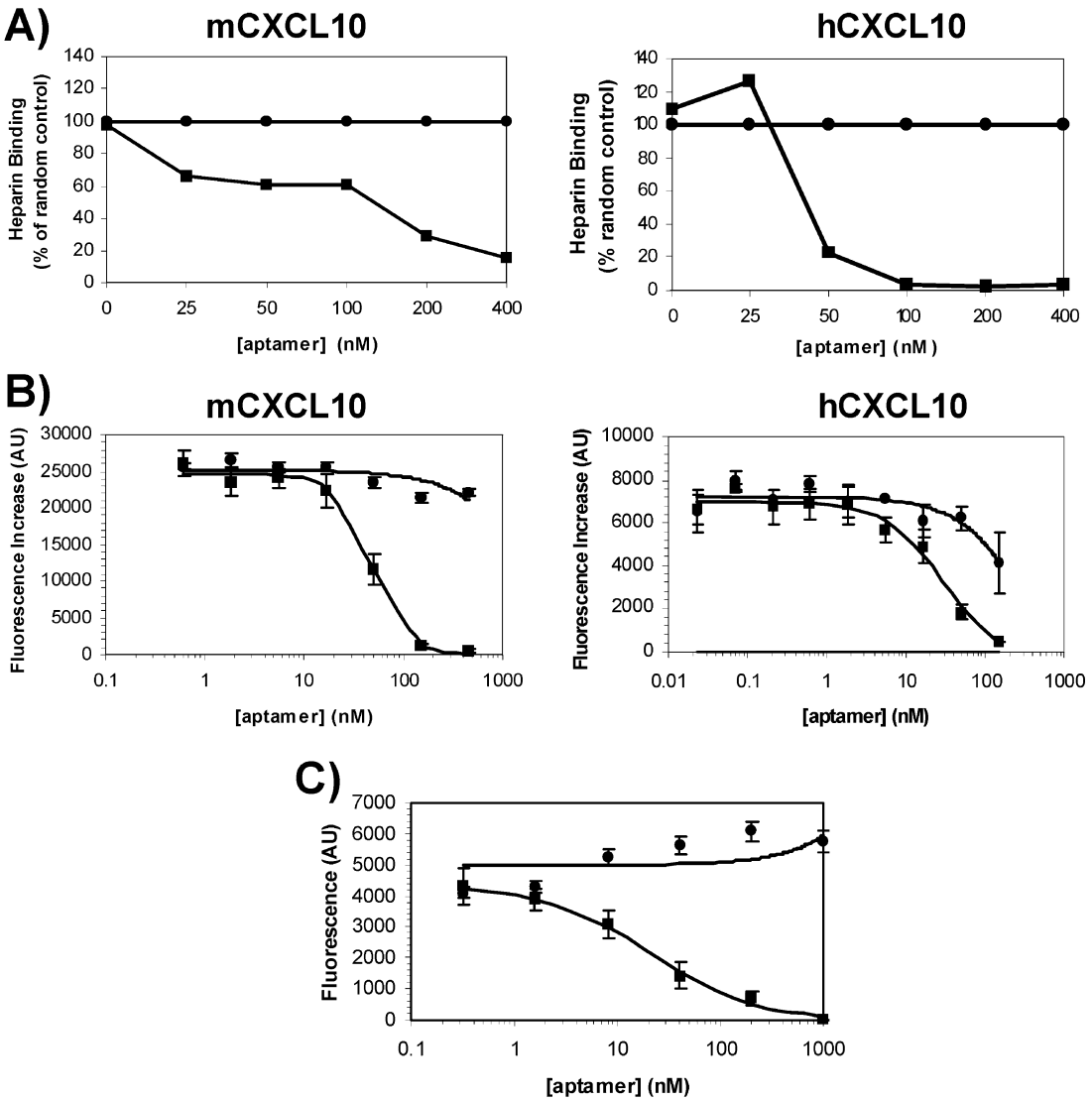

FIGURE 4: C44 aptamer is a potent antagonist of both mouse and human CXCL10. C44 aptamer (■) and a random control aptamer (●) are shown. (A) Aptamer blockade of heparin binding to mCXCL10 (left panel) and hCXCL10 (right panel) chemokines by using surface plasmon resonance. Each point represents the sensorgram peak in each case as a percentage of the random control one. (B) Aptamer inhibition of calcium mobilization in RBL cells expressing human CXCR3 by mCXCL10 (left panel) and hCXCL10 (right panel) chemokines. (C) Aptamer antagonism of hCXCL10-induced chemotaxis in human Th1 cells. (B, C) Experiments were carried out in triplicate. Error bars represent SE.

mCXCL10 aptamer is a potent antagonist of both mCXCL10 and hCXCL10 in at least two functional assays. Notably, the random aptamer showed no specific antagonism in any of the functional assays.

Optimization of the C44 Aptamer Molecule. (a) C44 Truncation. By generating progressively shorter oligonucleotides, it is possible to truncate active aptamers to identify the minimum functional element and consequently reduce future production costs. In this study, a molecular-biology-based truncation procedure was used in conjunction with solid-phase synthesis. Thus, serial 5′ and 3′ truncations in five nucleotide steps were carried out by PCR amplification followed by in vitro transcription and gel purification (Figure 5). A rational approach using secondary structure predictions drastically reduced the number of PCR-based truncates to be screened. The truncated RNAs were first tested against human and mouse CXCL10 in a calcium mobilization assay using RBL-CXCR3 cells at a single aptamer concentration (150 nM). The most potent aptamers (able to inhibit more than 90% of the calcium signaling) were then retested in the 0−450 nM range and demonstrated a dose-dependent inhibition. The best hCXCL10-specific C44 aptamer truncate was a 62-mer molecule (C44-62, Figure 6A). This truncated version contains 56 nucleotides of the original 71 nucleotide sequence plus 6 bases added to the 5′ end as part of the truncation strategy. Surprisingly, the potency of this shorter molecule increased 2−3-fold compared to that of the original C44 aptamer (data not shown). The best mCXCL10-specific aptamer truncate was a 47-mer molecule (C44-47). This aptamer was shown to be equipotent with the full-length C44 aptamer (IC_{50} = 40.2 nM, Figure 6A,B). Although P12 and P31 (described earlier) were shown to be potent anti-hCXCL10 antagonists, C44-62 might constitute a better candidate with therapeutic potential because it is derived from the same parent molecule (C44) truncated for target validation studies, generating C44-47.

(b) Addition of Chemical Modifications. Initial steps toward aptamer stabilization were taken by performing the SELEX methodology using 2′-fluoropyrimidines, which are known to provide a greater level of RNA stability to

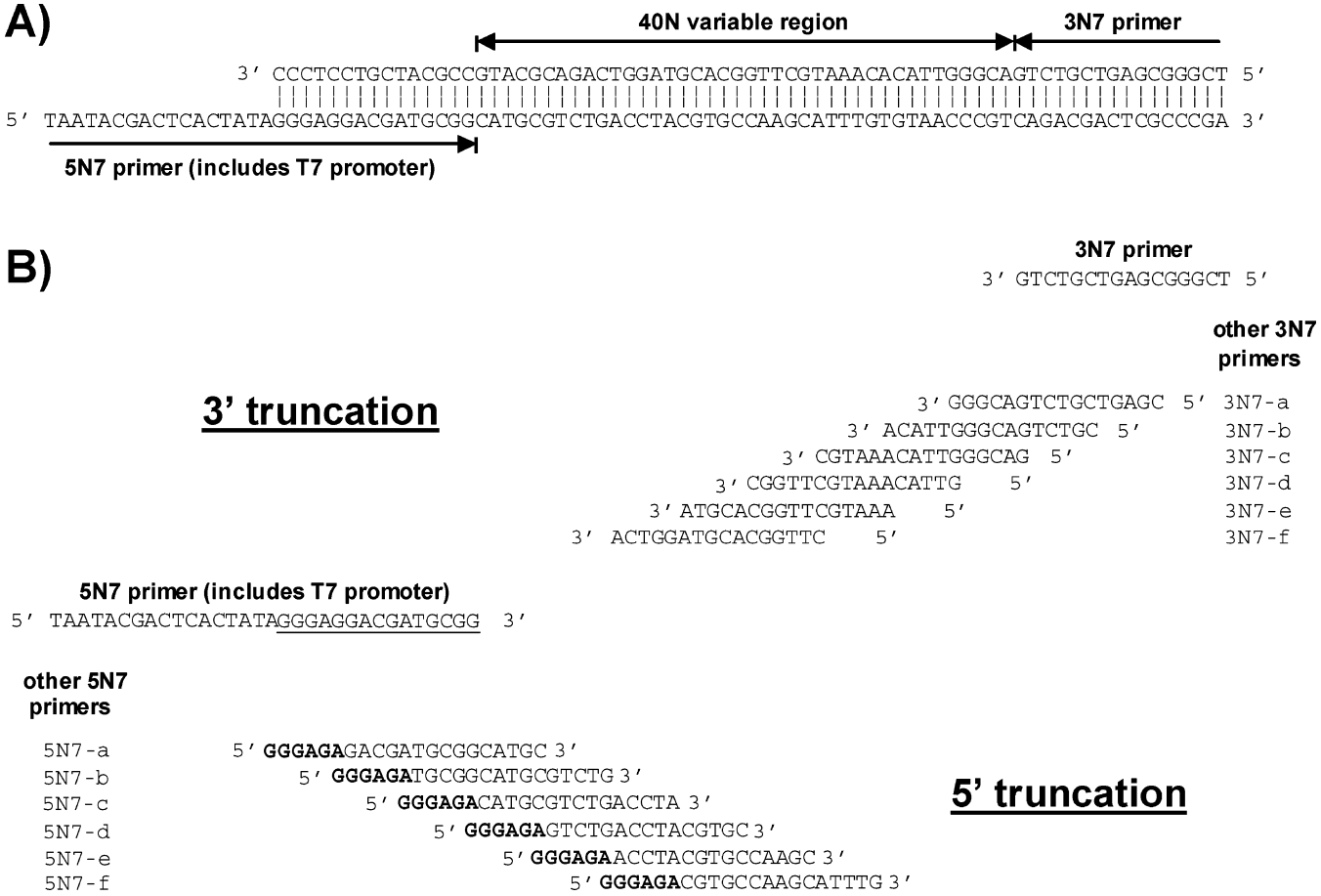

FIGURE 5: A molecular-biology-based strategy designed to truncate the C44 aptamer from both 5′ and 3′ ends. (A) The ds DNA sequence encoding the C44 cloned aptamer is shown together with the 5N7 and 3N7 primers utilized for the aptamer generation. (B) The set of all 5N7 and 3N7 primers utilized for the nested PCR from both ends is also shown. The T7 RNA polymerase promoter region is underlined in the 5N7 primer sequence. The GGGAGA region (boldface) at the 5′ end of each 5N7 primer constitutes the minimal region required for the T7 RNA polymerase promoter to be functional.

endonucleases. However, many additional chemical modifications have been described in the literature, some of which have been shown to be successful in stabilizing the aptamer molecules in cell-based assays or in vivo. After a careful analysis of those modifications present in the best in vivo RNA aptamers, a 40K PEG was added to the 5′ end of the truncated C44 aptamer via an N6 linker. We expected the linker would reduce the steric effects between the PEG group and the rest of the molecule as well as protect against 5′ exonucleases. Additionally, an idT was added to the 3′ end of the molecule to protect against 3′ exonucleases. To test whether these chemical groups might alter the original potency, a set of differentially modified C44-47 versions was synthesized and tested in an mCXCL10-induced calcium immobilization assay. The modifications were found not to dramatically alter the potency of the original C44-47 molecule (Table 3). Secondary structure prediction (data not shown) suggested that C44-47 could be shortened to 38 (C44-38) or 34 (C44-34) bases (Figure 6A), at the same time reducing any possible detrimental effect of appending the T7 promoter to the truncation fragments. To make the C44-34 structure more stable, a predicted U−A base pair, formed between the 5′ and 3′ ends of the molecule, was replaced by a G−C base pair. When the C44-38 aptamer was finally tested in an mCXCL10 calcium mobilization assay, it was shown to be slightly more potent than the C44-47 aptamer (IC_{50} = 29.3 nM, data not shown). Further addition of an N6 with or without PEGylation at the 5′ end of the C44-38 or the C44-34 molecule did not dramatically alter the potencies of these molecules (Table 3). Figure 6C depicts the concentration−response curves of the differentially modified C44 aptamers. In summary, the C44 aptamer has been truncated to less than half the size of the original molecule and has been chemically modified. This is likely to result in a substantial increase in the in vivo half-life without compromising potency. To ensure that the aptamer optimization did not alter the specificity, the PEGylated C44-34 aptamer was tested against the other two mCXCR3 ligands: mCXCL11 and mCXCL9. This aptamer did not specifically antagonize these ligands in a calcium mobilization assay (data not shown).

In conclusion, the evolution of the 71-mer aptamer C44 to the PEGylated 34-mer aptamer with the retention of high potency and specificity has resulted in the identification of an excellent candidate molecule for future studies of CXCL10/CXCR3 biology.

DISCUSSION

The elucidation of the role of chemokines and their receptors in both normal physiology and in disease states has previously been approached in different ways. The range of activity in the chemokine network is highly complex and involves several levels of redundancy. At present, there is a growing interest in unraveling the function of individual

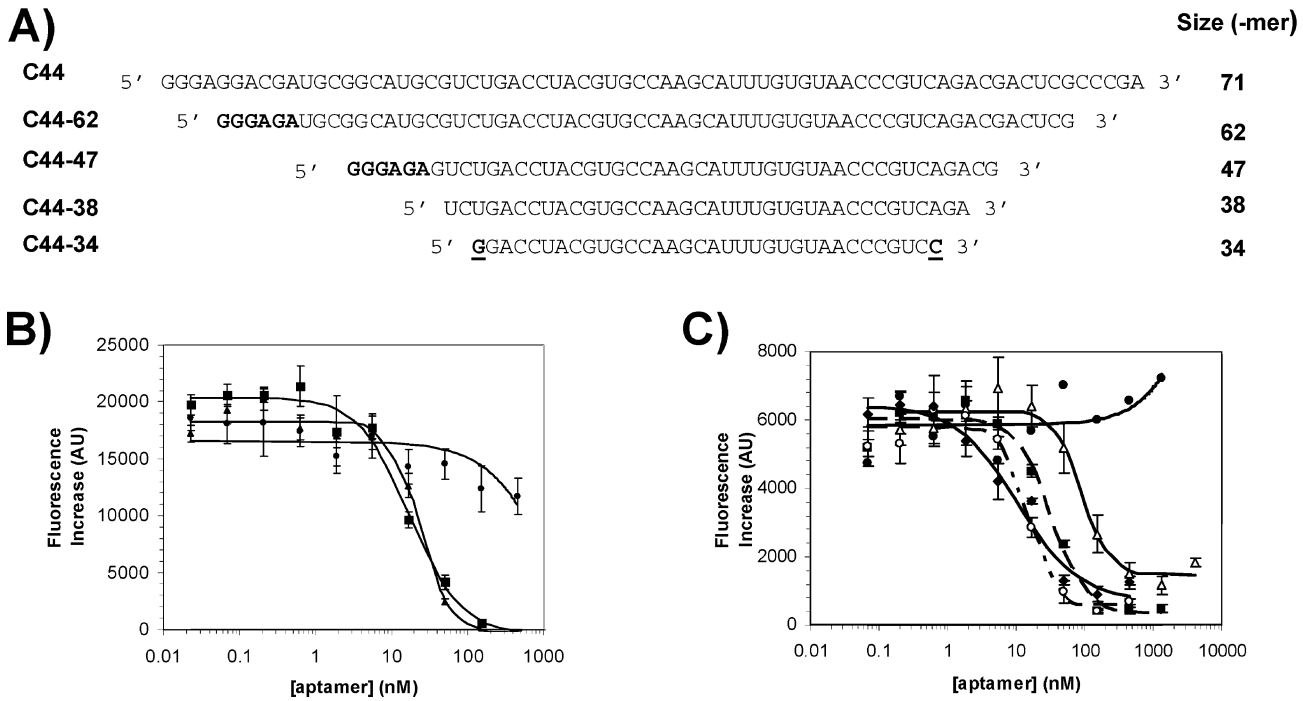

FIGURE 6: Screening and optimization of C44 truncates against hCXCL10 and mCXCL10. (A) C44 and C44-62 are antagonists of both hCXCL10 and mCXCL10. Further sequential truncation from 62 bases to 47, 38, and 34 bases generated 3 aptamers capable of antagonizing only mCXCL10. Underlined G and C bases replaced U and A bases, respectively (see below). (B) The C44-47 aptamer (■) was shown to be equipotent to C44 aptamer (▲) (IC_{50} = 40.2 nM) against mCXCL10. The random aptamer (●) did not show any response. (C) Different chemical modifications designed in the C44-47 molecule did not alter dramatically the potency of the naked molecule (see also Table 3). PEG-N6-C44-47-idT (△, solid line), N6-C44-47-idT (■, dashed line), C44-47-idT (○, dot chain), C44-47 (◆, solid line), and a random control (●, solid line) are shown. The hexamer introduced in the 5′ end of C44-62 and C44-47 aptamers as a consequence of maintaining the T7 promoter region is in boldface type (A). Experiments B and C were CXCL10-induced calcium mobilization assays and were carried out in triplicate. Error bars represent SE.

Table 3: Size, Length, and Potencies of the Different Chemically Modified Versions of the Truncated C44 Aptamers Produced by Dharmacon Research (Lafayette, CO)[a]

Aptamer	Chemical modifications	MW (kDa)	Length (nt)	IC50 (nM)
DH1	5' 40 kDa PEG-N6-C44-47-idT 3'	15.6	48	90.5
DH2	5' N6-C44-47-idT 3'	15.6	48	59.2
DH3	5' C44-47-idT 3'	15.5	48	47.5
DH4	5' C44-47 3'	15.2	47	45.8
C44-47	5' C44-47 3'	15.2	47	37.5
DH6	5' 40 kDa PEG- N6-C44-38-idT 3'	12.6	39	72.0
DH7	5' N6-C44-38-idT 3'	12.6	39	46.0
DH8	5' 40 kDa PEG- N6-C44-34-idT 3'	11.3	35	75.5
DH9	5' N6-C44-34-idT 3'	11.3	35	43.4

[a] Potencies were estimated in an mCXCL10-induced calcium mobilization assay using the RBL-CXCR3 cell line. DH4 represents the chemically synthesized version of C44-47, utilized as a positive control of the chemical synthesis.

chemokine ligands. In the case of CXCR3 receptors, CXCL10 expression is sometimes regulated differently from CXCL11 and CXCL9, as shown in an allograft rejection model (*49*−*51*). Thus, while chemokine receptors may bind multiple chemokines, a specific ligand−receptor interaction may be important in particular physiological and pathological conditions. This highlights the importance of validating the chemokine ligands individually or in combination to understand their biological role in a specific situation (*25*).

To complement gene knockout and antisense technologies, techniques have been developed that allow the generation of specific peptide or nucleotide aptamers to target proteins. In contrast to antibody generation, aptamers can be produced rapidly using an in vitro selection procedure. In this study, we have focused on the generation and characterization of RNA aptamers to better understand the biological function of CXCL10. We report here the isolation of a series of RNA aptamers with high binding affinity for human and/or mouse CXCL10 that act to antagonize CXCL10 function in a number of in vitro and cell-based assays.

An important step in chemokine-mediated leukocyte recruitment is the immobilization of the chemokines on cell surface GAGs (*25*). Campanella et al recently found that the N-terminal residue (*52*) as well as residues in the loop regions (20−24 and 46−47) of the mCXCL10 chemokine were important for CXCR3 binding. Interestingly, these same loop regions together with K26 were also the major heparin binding site, suggesting that the CXCR3 and heparin binding sites of CXCL10 were partially overlapping (*47*). Since anti-hCXCL10 aptamers (P12, P31, and C44) and the anti-mCXCL10 aptamers (C44) block not only heparin binding in vitro but also CXCR3 binding and activity (Figures 2 and 4; Supporting Information, Figure 8), these molecules might bind either to these loop regions alone or in addition to several other regions of the CXCL10 molecule.

P12 and P31 were shown to be potent antagonists of hCXCL10 function in different cell-based assays, showing a very good correlation in activity (Table 2). Although hCXCL10 shares ∼37% identity with hCXCL9 and hCXCL11, neither P12 nor P31 specifically antagonized

these chemokines (Figure 3A,B). The strong selectivity of P12 and P31 aptamers is demonstrated by the fact that they did not antagonize the mCXCL10 ligand (Figure 3D), despite being 70% identical to hCXCL10. This striking selectivity suggested the aptamers could specifically discriminate against other chemokines less related to hCXCL10 than mCXCL10. This was demonstrated by the observation that when two CC-chemokines, CCL1 and CCL22, were tested, P12 and P31 aptamers did not block their activity (Supporting Information, Figure 9). In summary, these RNA molecules are not only potent but also very specific and selective antagonists of their target.

The C44 aptamer was the only RNA molecule identified capable of antagonizing both the human and the mouse CXCL10, making this aptamer an excellent tool for target validation and potentially a candidate for therapeutic use. This aptamer was shown to be functional in assays against both mouse and human CXCL10 (Figure 4).

The optimization of aptamers for in vivo studies involves a truncation step that is crucial to reduce large-scale production costs of aptamers. Commonly, aptamer truncation is performed using solid-phase synthesis. Here, we have introduced a strategy where the truncation procedure was biological, by using nested PCRs followed by in vitro transcription and purification (Figure 5). Although this procedure was successful and less expensive than the production of multiple truncates through chemical synthesis, for the final truncation steps, we complemented it with a chemical truncation approach. This was done primarily to eliminate the potential detrimental effect of appending the T7 promoter region to each truncation fragment. Thus, we eliminated five out of six bases from the promoter in the final 34-base version.

Some attempts to optimize aptamers for in vivo studies have resulted in a loss of affinity or potency throught either truncation or addition of post-SELEX chemical modifications (*53*, *54*). We have successfully truncated the 71-mer C44 molecule to a 38-mer, maintaining the original potency. Moreover, the further truncation to less than half of the original length (34-mer), PEGylation, N6 addition, and capping at the 3′ end only slightly altered the original potency of C44 (Table 3).

The cross-talk between the CXCL10/CXCR3 receptor and other chemokine/receptor systems is illustrated in several papers. First, CXCR3 ligands such as CXCL10 can also antagonize the CCR3 receptor (*55*). At the same time, CCL11 (and also CCL13) bind with high affinity and antagonize the CXCR3 receptor (*56*). Second, CXCL13 has been reported to also bind CXCR3, in addition to its previously known partner CXCR5 (*57*). Finally, mouse CCL21, the usual CXCR5 ligand, can signal through CXCR3 (*58*), despite human CCL21 not being a ligand for the human or mouse CXCR3 receptors (*59*). This complicated interplay of interactions may serve to finely tune inflammatory responses in vivo. We believe that these aptamers could be utilized as powerful target validation tools able to dissect CXCL10-specific function.

In summary, we report here the isolation of a series of nuclease-resistant and selective RNA aptamers with high binding affinity for human and/or mouse CXCL10 that act to antagonize CXCL10 function in a number of in vitro and cell-based assays. These aptamers might represent powerful target validation tools, and they could also be beneficial in situations where exaggerated CXCL10 synthesis is harmful and therefore may also have potential as therapeutic tools in their own right. To our knowledge, the CXCL10 aptamers are the most potent antagonists reported to date at the CXCL10/CXCR3 signaling axis.

ACKNOWLEDGMENT

We thank Simon Dowell for critically reading the paper and for his support. We are grateful to Ashley Barnes for his helpful discussions and to Andrew Rhodes for his ideas about aptamer characterization. We also thank Elizabeth Capper for her support and useful comments about the CXCR3/CXCL10 axis.

SUPPORTING INFORMATION AVAILABLE

One figure with nitrocellulose binding assays of the P12 and P31 aptamers, two figures showing a rightward shift in the agonist concentration−response curve (cAMP assay) by these aptamers at two different concentrations, and two figures with P12 and P31 aptamers showing no effect on CCL1 and CCL22 chemokines. This material is available free of charge via the Internet at http://pubs.acs.org.

REFERENCES

1. Luster, A. D. and Ravetch, J. V. (1987) Genomic characterization of a gamma-interferon-inducible gene (IP-10) and identification of an interferon-inducible hypersensitive site, *Mol. Cell Biol. 7* (10), 3723−3731.
2. Luster, A. D. (1998) Chemokines—chemotactic cytokines that mediate inflammation, *N. Engl. J. Med. 338* (7), 436−445.
3. Gattass, C. R., King, L. B., Luster, A. D., and Ashwell, J. D. (1994) Constitutive expression of interferon gamma-inducible protein 10 in lymphoid organs and inducible expression in T cells and thymocytes, *J. Exp. Med. 179* (4), 1373−1378.
4. Luster, A. D., Unkeless, J. C., and Ravetch, J. V. (1985) Gamma-interferon transcriptionally regulates an early-response gene containing homology to platelet proteins, *Nature 315* (6021), 672−676.
5. Luster, A. D. and Ravetch, J. V. (1987) Biochemical characterization of a gamma interferon-inducible cytokine (IP-10), *J. Exp. Med. 166* (4), 1084−1097.
6. Flier, J., Boorsma, D. M., Bruynzeel, D. P., Van Beek, P. J., Stoof, T. J., Scheper, R. J., Willemze, R., and Tensen, C. P. (1999) The CXCR3 activating chemokines IP-10, Mig, and IP-9 are expressed in allergic but not in irritant patch test reactions, *J. Invest. Dermatol. 113* (4), 574−578.
7. Flier, J., Boorsma, D. M., Van Beek, P. J., Nieboer, C., Stoof, T. J., Willemze, R., and Tensen, C. P. (2001) Differential expression of CXCR3 targeting chemokines CXCL10, CXCL9, and CXCL11 in different types of skin inflammation, *J. Pathol. 194* (4), 398−405.
8. Gottlieb, A. B., Luster, A. D., Posnett, D. N., and Carter, D. M. (1988) Detection of a gamma interferon-induced protein IP-10 in psoriatic plaques, *J. Exp. Med. 168* (3), 941−948.
9. Mach, F., Sauty, A., Iarossi, A. S., Sukhova, G. K., Neote, K., Libby, P., and Luster, A. D. (1999) Differential expression of three T lymphocyte-activating CXC chemokines by human atheroma-associated cells, *J. Clin. Invest. 104* (8), 1041−1050.
10. Balashov, K. E., Rottman, J. B., Weiner, H. L., and Hancock, W. W. (1999) CCR5(+) and CXCR3(+) T cells are increased in multiple sclerosis and their ligands MIP-1alpha and IP-10 are expressed in demyelinating brain lesions, *Proc. Natl. Acad. Sci. U.S.A. 96* (12), 6873−6878.
11. Sorensen, T. L., Tani, M., Jensen, J., Pierce, V., Lucchinetti, C., Folcik, V. A., Qin, S., Rottman, J., Sellebjerg, F., Strieter, R. M., Frederiksen, J. L., and Ransohoff, R. M. (1999) Expression of specific chemokines and chemokine receptors in the central nervous system of multiple sclerosis patients, *J. Clin. Invest. 103* (6), 807−815.

12. Jiankuo, M., Xingbing, W., Baojun, H., Xiongwin, W., Zhuoya, L., Ping, X., Yong, X., Anting, L., Chunsong, H., Feili, G., and Jinquan, T. (2003) Peptide nucleic acid antisense prolongs skin allograft survival by means of blockade of CXCR3 expression directing T cells into graft, *J. Immunol. 170* (3), 1556−1565.
13. Zhao, D. X., Hu, Y., Miller, G. G., Luster, A. D., Mitchell, R. N., and Libby, P. (2002) Differential expression of the IFN-gamma-inducible CXCR3-binding chemokines, IFN-inducible protein 10, monokine induced by IFN, and IFN-inducible T cell alpha chemoattractant in human cardiac allografts: association with cardiac allograft vasculopathy and acute rejection, *J. Immunol. 169* (3), 1556−1560.
14. Angiolillo, A. L., Sgadari, C., Taub, D. D., Liao, F., Farber, J. M., Maheshwari, S., Kleinman, H. K., Reaman, G. H., and Tosato, G. (1995) Human interferon-inducible protein 10 is a potent inhibitor of angiogenesis in vivo, *J. Exp. Med. 182* (1), 155−162.
15. Luster, A. D., Greenberg, S. M., and Leder, P. (1995) The IP-10 chemokine binds to a specific cell surface heparan sulfate site shared with platelet factor 4 and inhibits endothelial cell proliferation, *J. Exp. Med. 182* (1), 219−231.
16. Sgadari, C., Angiolillo, A. L., and Tosato, G. (1996) Inhibition of angiogenesis by interleukin-12 is mediated by the interferon-inducible protein 10, *Blood 87* (9), 3877−3882.
17. Strieter, R. M., Kunkel, S. L., Arenberg, D. A., Burdick, M. D., and Polverini, P. J. (1995) Interferon gamma-inducible protein 10 (IP-10), a member of the C-X-C chemokine family, is an inhibitor of angiogenesis, *Biochem. Biophys. Res. Commun. 210* (1), 51−57.
18. Arenberg, D. A., Kunkel, S. L., Polverini, P. J., Morris, S. B., Burdick, M. D., Glass, M. C., Taub, D. T., Iannettoni, M. D., Whyte, R. I., and Strieter, R. M. (1996) Interferon-gamma-inducible protein 10 (IP-10) is an angiostatic factor that inhibits human non-small cell lung cancer (NSCLC) tumorigenesis and spontaneous metastases, *J. Exp. Med. 184* (3), 981−992.
19. Luster, A. D. and Leder, P. (1993) IP-10, a −C-X-C- chemokine, elicits a potent thymus-dependent antitumor response in vivo, *J. Exp. Med. 178* (3), 1057−1065.
20. Sasaki, S., Yoneyama, H., Suzuki, K., Suriki, H., Aiba, T., Watanabe, S., Kawauchi, Y., Kawachi, H., Shimizu, F., Matsushima, K., Asakura, H., and Narumi, S. (2002) Blockade of CXCL10 protects mice from acute colitis and enhances crypt cell survival, *Eur. J. Immunol. 32* (11), 3197−3205.
21. Thomas, M. S., Kunkel, S. L., and Lukacs, N. W. (2002) Differential role of IFN-gamma-inducible protein 10 kDa in a cockroach antigen-induced model of allergic airway hyperreactivity: systemic versus local effects, *J. Immunol. 169* (12), 7045−7053.
22. Lane, B. R., King, S. R., Bock, P. J., Strieter, R. M., Coffey, M. J., and Markovitz, D. M. (2003) The C−X-C chemokine IP-10 stimulates HIV-1 replication, *Virology 307* (1), 122−134.
23. Loetscher, M., Loetscher, P., Brass, N., Meese, E., and Moser, B. (1998) Lymphocyte-specific chemokine receptor CXCR3: regulation, chemokine binding and gene localization, *Eur. J. Immunol. 28* (11), 3696−3705.
24. Booth, V., Keizer, D. W., Kamphuis, M. B., Clark-Lewis, I., and Sykes, B. D. (2002) The CXCR3 binding chemokine IP-10/CXCL10: structure and receptor interactions, *Biochemistry 41* (33), 10418−10425.
25. Proudfoot, A. E., Power, C. A., Rommel, C., and Wells, T. N. (2003) Strategies for chemokine antagonists as therapeutics, *Semin. Immunol. 15* (1), 57−65.
26. Dufour, J. H., Dziejman, M., Liu, M. T., Leung, J. H., Lane, T. E., and Luster, A. D. (2002) IFN-gamma-inducible protein 10 (IP-10; CXCL10)-deficient mice reveal a role for IP-10 in effector T cell generation and trafficking, *J. Immunol. 168* (7), 3195−3204.
27. Khan, I. A., MacLean, J. A., Lee, F. S., Casciotti, L., DeHaan, E., Schwartzman, J. D., and Luster, A. D. (2000) IP-10 is critical for effector T cell trafficking and host survival in Toxoplasma gondii infection, *Immunity 12* (5), 483−494.
28. Zhang, Z., Kaptanoglu, L., Haddad, W., Ivancic, D., Alnadjim, Z., Hurst, S., Tishler, D., Luster, A. D., Barrett, T. A., and Fryer, J. (2002) Donor T cell activation initiates small bowel allograft rejection through an IFN-gamma-inducible protein-10-dependent mechanism, *J. Immunol. 168* (7), 3205−3212.
29. Baker, M. S., Chen, X., Rotramel, A. R., Nelson, J. J., Lu, B., Gerard, C., Kanwar, Y., and Kaufman, D. B. (2003) Genetic deletion of chemokine receptor CXCR3 or antibody blockade of its ligand IP-10 modulates posttransplantation graft-site lymphocytic infiltrates and prolongs functional graft survival in pancreatic islet allograft recipients, *Surgery 134* (2), 126−133.
30. Tuerk, C. and Gold, L. (1990) Systematic evolution of ligands by exponential enrichment: RNA ligands to bacteriophage T4 DNA polymerase, *Science 249* (4968), 505−510.
31. Fitzwater, T. and Polisky, B. (1996) A SELEX primer, *Methods Enzymol. 267*275−301.
32. Gold, L., Polisky, B., Uhlenbeck, O., and Yarus, M. (1995) Diversity of oligonucleotide functions, *Annu. Rev. Biochem. 64*763−797.
33. Ellington, A. D. and Szostak, J. W. (1990) In vitro selection of RNA molecules that bind specific ligands, *Nature 346* (6287), 818−822.
34. Brody, E. N. and Gold, L. (2000) Aptamers as therapeutic and diagnostic agents, *J. Biotechnol. 74* (1), 5−13.
35. Famulok, M., Mayer, G., and Blind, M. (2000) Nucleic acid aptamers-from selection in vitro to applications in vivo, *Acc. Chem. Res. 33* (9), 591−599.
36. Rhodes, A., Deakin, A., Spaull, J., Coomber, B., Aitken, A., Life, P., and Rees, S. (2000) The generation and characterization of antagonist RNA aptamers to human oncostatin M, *J. Biol. Chem. 275* (37), 28555−28561.
37. Rhodes, A., Smithers, N., Chapman, T., Parsons, S., and Rees, S. (2001) The generation and characterisation of antagonist RNA aptamers to MCP-1, *FEBS Lett. 506* (2), 85−90.
38. Burgstaller, P., Jenne, A., and Blind, M. (2002) Aptamers and aptazymes: accelerating small molecule drug discovery, *Curr. Opin. Drug Discovery Dev. 5* (5), 690−700.
39. Daniels, D. A., Sohal, A. K., Rees, S., and Grisshammer, R. (2002) Generation of RNA aptamers to the G-protein-coupled receptor for neurotensin, NTS-1, *Anal. Biochem. 305* (2), 214−226.
40. Zuker, M. (2003) Mfold web server for nucleic acid folding and hybridization prediction, *Nucleic Acids Res. 31* (13), 3406−3415.
41. Sullivan, E., Tucker, E. M., and Dale, I. L. (1999) Measurement of [Ca2+] using the Fluorometric Imaging Plate Reader (FLIPR), *Methods Mol. Biol. 114*125−133.
42. Andrew, D. P., Ruffing, N., Kim, C. H., Miao, W., Heath, H., Li, Y., Murphy, K., Campbell, J. J., Butcher, E. C., and Wu, L. (2001) C-C chemokine receptor 4 expression defines a major subset of circulating nonintestinal memory T cells of both Th1 and Th2 potential, *J. Immunol. 166* (1), 103−111.
43. Hoogewerf, A. J., Kuschert, G. S., Proudfoot, A. E., Borlat, F., Clark-Lewis, I., Power, C. A., and Wells, T. N. (1997) Glycosaminoglycans mediate cell surface oligomerization of chemokines, *Biochemistry 36* (44), 13570−13578.
44. Tanaka, Y., Adams, D. H., Hubscher, S., Hirano, H., Siebenlist, U., and Shaw, S. (1993) T-cell adhesion induced by proteoglycan-immobilized cytokine MIP-1 beta, *Nature 361* (6407), 79−82.
45. Chang, T. L., Gordon, C. J., Roscic-Mrkic, B., Power, C., Proudfoot, A. E., Moore, J. P., and Trkola, A. (2002) Interaction of the CC-chemokine RANTES with glycosaminoglycans activates a p44/p42 mitogen-activated protein kinase-dependent signaling pathway and enhances human immunodeficiency virus type 1 infectivity, *J. Virol. 76* (5), 2245−2254.
46. Fleischer, J., Grage-Griebenow, E., Kasper, B., Heine, H., Ernst, M., Brandt, E., Flad, H. D., and Petersen, F. (2002) Platelet factor 4 inhibits proliferation and cytokine release of activated human T cells, *J. Immunol. 169* (2), 770−777.
47. Campanella, G. S., Lee, E. M., Sun, J., and Luster, A. D. (2003) CXCR3 and heparin binding sites of the chemokine IP-10 (CXCL10), *J. Biol. Chem. 278* (19), 17066−17074.
48. Cole, K. E., Strick, C. A., Paradis, T. J., Ogborne, K. T., Loetscher, M., Gladue, R. P., Lin, W., Boyd, J. G., Moser, B., Wood, D. E., Sahagan, B. G., and Neote, K. (1998) Interferon-inducible T cell alpha chemoattractant (I-TAC): a novel non-ELR CXC chemokine with potent activity on activated T cells through selective high affinity binding to CXCR3, *J. Exp. Med. 187* (12), 2009−2021.
49. Hancock, W. W., Lu, B., Gao, W., Csizmadia, V., Faia, K., King, J. A., Smiley, S. T., Ling, M., Gerard, N. P., and Gerard, C. (2000) Requirement of the chemokine receptor CXCR3 for acute allograft rejection, *J. Exp. Med. 192* (10), 1515−1520.
50. Kao, J., Kobashigawa, J., Fishbein, M. C., MacLellan, W. R., Burdick, M. D., Belperio, J. A., and Strieter, R. M. (2003) Elevated serum levels of the CXCR3 chemokine ITAC are associated with the development of transplant coronary artery disease, *Circulation 107* (15), 1958−1961.
51. Salmaggi, A., Gelati, M., Dufour, A., Corsini, E., Pagano, S., Baccalini, R., Ferrero, E., Scabini, S., Silei, V., Ciusani, E., and De Rossi, M. (2002) Expression and modulation of IFN-gamma-

inducible chemokines (IP-10, Mig, and I-TAC) in human brain endothelium and astrocytes: possible relevance for the immune invasion of the central nervous system and the pathogenesis of multiple sclerosis, *J. Interferon Cytokine Res. 22* (6), 631−640.
52. Goya, I., Villares, R., Zaballos, A., Gutierrez, J., Kremer, L., Gonzalo, J. A., Varona, R., Carramolino, L., Serrano, A., Pallares, P., Criado, L. M., Kolbeck, R., Torres, M., Coyle, A. J., Gutierrez-Ramos, J. C., Martinez, A., and Marquez, G. (2003) Absence of CCR8 does not impair the response to ovalbumin-induced allergic airway disease, *J. Immunol. 170* (4), 2138−2146.
53. Ruckman, J., Green, L. S., Beeson, J., Waugh, S., Gillette, W. L., Henninger, D. D., Claesson-Welsh, L., and Janjic, N. (1998) 2′-Fluoropyrimidine RNA-based aptamers to the 165-amino acid form of vascular endothelial growth factor (VEGF165). Inhibition of receptor binding and VEGF-induced vascular permeability through interactions requiring the exon 7-encoded domain, *J. Biol. Chem. 273* (32), 20556−20567.
54. Watson, S. R., Chang, Y. F., O'Connell, D., Weigand, L., Ringquist, S., and Parma, D. H. (2000) Anti-L-selectin aptamers: binding characteristics, pharmacokinetic parameters, and activity against an intravascular target in vivo, *Antisense Nucleic Acid Drug Dev. 10* (2), 63−75.
55. Loetscher, P., Pellegrino, A., Gong, J. H., Mattioli, I., Loetscher, M., Bardi, G., Baggiolini, M., and Clark-Lewis, I. (2001) The ligands of CXC chemokine receptor 3, I.-TAC, Mig, and IP10, are natural antagonists for CCR3, *J. Biol. Chem. 276* (5), 2986−2991.
56. Xanthou, G., Duchesnes, C. E., Williams, T. J., and Pease, J. E. (2003) CCR3 functional responses are regulated by both CXCR3 and its ligands CXCL9, CXCL10 and CXCL11, *Eur. J. Immunol. 33* (8), 2241−2250.
57. Jenh, C. H., Cox, M. A., Hipkin, W., Lu, T., Pugliese-Sivo, C., Gonsiorek, W., Chou, C. C., Narula, S. K., and Zavodny, P. J. (2001) Human B cell-attracting chemokine 1 (BCA-1; CXCL13) is an agonist for the human CXCR3 receptor, *Cytokine 15* (3), 113−121.
58. Soto, H., Wang, W., Strieter, R. M., Copeland, N. G., Gilbert, D. J., Jenkins, N. A., Hedrick, J., and Zlotnik, A. (1998) The CC chemokine 6Ckine binds the CXC chemokine receptor CXCR3, *Proc. Natl. Acad. Sci. U.S.A. 95* (14), 8205−8210.
59. Jenh, C. H., Cox, M. A., Kaminski, H., Zhang, M., Byrnes, H., Fine, J., Lundell, D., Chou, C. C., Narula, S. K., and Zavodny, P. J. (1999) Cutting edge: species specificity of the CC chemokine 6Ckine signaling through the CXC chemokine receptor CXCR3: human 6Ckine is not a ligand for the human or mouse CXCR3 receptors, *J. Immunol. 162* (7), 3765−3769.

BI048145W